

# How cryptic is cryptic diversity? Machine learning approaches to classifying morphological variation in *Emys marmorata* (Testudinoidea, Emydidae).

Peter D Smits<sup>1</sup>, Kenneth D Angielczyk<sup>1,2</sup>, and James F Parham<sup>3</sup>

<sup>1</sup>Committee on Evolutionary Biology, University of Chicago

<sup>2</sup>Integrative Research Center, Field Museum of Natural History

<sup>3</sup>Department of Geological Sciences, California State University – Fullerton

August 5, 2015

**Corresponding author:** Peter D Smits, Committee on Evolutionary Biology, University of Chicago, 1025 E. 57th Street, Culver Hall 402, Chicago, IL, 60637, USA; E-mail: psmits@uchicago.edu

## Abstract

2

## INTRODUCTION

4 With the rise of molecular systematics and techniques such as DNA barcoding, it has been  
increasingly recognized that some taxa can only be differentiated using molecular data  
6 (Bickford et al. 2007; Clare 2011; Funk et al. 2012; Pfenninger and Schwenk 2007; Schilck-  
Steiner et al. 2007; Stuart et al. 2006). Nevertheless, the majority of extant taxa, and nearly  
8 all extinct taxa, are delimited solely via morphology. This disjunct is of great concern for  
studies of variation and diversity dynamics in deep time, where apparent morphological stasis  
10 may not reflect the true underlying diversity that existed (Eldredge and Gould 1972; Gould  
and Eldredge 1977; Hunt 2008; Van Bocxlaer and Hunt 2013).

12 Much work has been devoted to species delimitation via sequence difference (Fujita et al.  
2012; Yang and Rannala 2010) which in turn has sparked interest in whether geometric  
14 morphometric analysis can capture similarly fine-scale variation that can be used for identifying  
cryptic species. Most such studies focus on morphometrics to discover differences between  
16 taxa that were identified by other means (Demandt and Bergek 2009; Gaubert et al. 2005;  
Gündüz et al. 2007; Polly 2003, 2007; Zelditch et al. 2004) and automated taxon identification

(MacLeod 2007). It would be very useful, though, if morphometrics approaches could reliably identify cryptic species without the use of other types of data. This would make the task of identifying and maintaining endangered or conserved groups much easier and could contribute to improved classifications of extinct taxa.

Here, we attempt to address this issue using machine learning approaches. In particular, we ask whether it is possible to determine which amongst a set of classification hypotheses is best and examine the implications of the results for a recently proposed set of cryptic turtle species.

## *Background and system*

Machine learning is in many respects just an extension of known statistical methodology (Hastie et al. 2009) in which the emphasis is placed on high predictive accurate at the expense of interpretability of individual parameters. The basic statistical mechanics are supplemented by randomization, sorting, and partitioning algorithms and along with the maximization or minimization of summary statistics, in order to best estimate a general model for all data, both sampled and unsampled (Hastie et al. 2009). Machine learning approaches have found use in medical research, epidemiology, economics and automated image identification such as handwritten zip codes (Hastie et al. 2009). Two major classes of machine learning methods are unsupervised and supervised learning. Unsupervised learning methods are used with unlabeled data where the underlying structure is estimated and are analogous to clustering and density estimation methods (Kaufman and Rousseeuw 1990). Supervised learning methods are used with labeled data where the final output of data is known and the rules for going from input to output are inferred. These are analogous classification and regression models (Breiman et al. 1984). The application of the alternative approaches used in this study illustrates only a sampling of the various previously derived methods for clustering observations and fitting classification models.

Geometric morphometric approaches to identifying differences in morphological variation between different classes, including cryptic species, mostly have used methods like linear discriminate analysis and canonical variates analysis (Demandt and Bergek 2009; Francoy et al. 2009; Gaubert et al. 2005; Gündüz et al. 2007; Mitrovski-Bogdanovic et al. 2013; Mitteroecker and Bookstein 2011; Polly 2003, 2007; Sztencel-Jabonka et al. 2009; Zelditch et al. 2004). These methods are comparatively straightforward ways of understanding the differences in morphology between classes given their similarity to familiar multivariate approaches like principal components analysis (PCA). They are benefit by producing results that can be easily visualized, which aids in the interpretation and presentation of data and results. Most previous morphometric studies did not assess which amongst a set of alternative classification hypotheses was optimal. For example, studies such as those of Caumul and Polly (2005) and Polly (2007) focused on comparing different aspects of morphology and their fidelity to a classification scheme instead of comparing the fidelity of one aspect of morphology to multiple classification schemes. In this context, the study of Cardini et al. (2009), is noteworthy because they compared morphological variation in marmots at the

population, regional, and species level and determined the fidelity of shape to divisions at each of these levels.

Here, we used multiple machine learning methods, both unsupervised and supervised, in order to compare different classification hypotheses. These methods provide different and unique advantages for understanding how to classify taxa, and with what accuracy. While machine learning methods such as neural networks have been applied to studying shape variation (Baylac et al. 2003; Dobigny et al. 2003; MacLeod 2007; van den Brink and Bokma 2011), including in the context of automated taxon identification and classification of groups, the number of cases remains limited. In the current study, we not only consider pure classification accuracy but also use a statistic of classification strength that reflects the rate at which taxa are both accurately and inaccurately classified.

### *Emys marmorata*

We analyzed the problem of whether there are distinct subspecies or cryptic species exist within the western pond turtle, *Emys marmorata* (formerly *Clemmys marmorata*; see Feldman and Parham 2002). *E. marmorata* is distributed from northern Washington State, USA to Baja California, Mexico. Traditionally, *E. marmorata* was classified into two named subspecies: the northern *E. marmorata marmorata*, the southern *E. marmorata palida* (Seeliger 1945). She also recognized a central Californian intergrade zone between these subspecies, and did not include the Baja California populations of *E. marmorata* in these groups, implying the existence of a third distinct but unnamed subspecies. *E. marmorata marmorata* is differentiated from *E. marmorata palida* by the presence of a pair of triangular inguinal plates and darker neck markings. It should be noted that the triangular inguinal plates can sometimes be present in *E. marmorata palida* though they are considerably smaller.

Previous work on morphological variation in *E. marmorata* has focused primarily on differentiation between populations over a portion of the species' total range (Bury et al. 2010; Germano and Bury 2009; Germano and Rathbun 2008; Lubcke and Wilson 2007); comparatively few studies have included specimens from across the entire range (Holland 1992). Most of these studies considered how local biotic and abiotic factors may contribute to differences in carapace length and found that size can vary greatly between different populations (Germano and Bury 2009; Germano and Rathbun 2008; Lubcke and Wilson 2007). There also has been interest in size-based sexual dimorphism in *E. marmorata* (Germano and Bury 2009; Holland 1992; Lubcke and Wilson 2007), with males being on average larger than females based on total carapace length and other linear measurements. However, the quality of size as a classifier of sex can vary greatly between populations (Holland 1992), which makes sense in light of the amount of between population size difference (Germano and Bury 2009; Lubcke and Wilson 2007). However, the effect of sexual dimorphism on shape, *sensu* Kendall (1977), was not assessed (Germano and Rathbun 2008; Holland 1992; Lubcke and Wilson 2007).

Of particular importance in the context of cryptic diversity in *E. marmorata* is the traditional morphometric analysis of carapace shape carried out by Holland (1992). He compared

morphological differences between and among many populations of *E. marmorata* in three different areas of the species' range, and studied the relative effect of distance versus barriers in fostering morphological differentiation in the species. Holland (1992) concluded that geographic distance was a poor indicator of morphological differentiation, and instead geographic features such as breaks between different drainage basins are probably more important barriers to reproduction. Additionally, Holland (1992) found that morphological differences were observable as the magnitude of barriers and distance increased, but the variation required many variables to adequately capture, implying only very subtle morphological differentiation between putatively distinct populations. Holland (1992) concluded that *E. marmorata* is best classified as three distinct species: a northern species, southern species, and a Columbia basin species. This classification is similar to that of Seeliger (1945), except elevated to the species level and without recognition of a distinct Baja species.

More recently, the phylogeography of *E. marmorata* and the possibility of cryptic diversity has been investigated using molecular data (Spinks and Shaffer 2005; Spinks et al. 2014, 2010). Based on mitochondrial DNA, Spinks and Shaffer (2005) recognized four subclades within *E. marmorata*, a northern clade, a San Joaquin Valley clade, a Santa Barbara clade, and a southern clade. Analyses with nuclear DNA (Spinks et al. 2010) with single-nucleotide polymorphism (SNP) data suggest a primarily north-south division in *E. marmorata*, although the dataset differs in the location of this break point. In these papers, Spinks and colleagues discussed the potential taxonomic implications of their results, with Spinks et al. (2014) going so far as to strongly advocate for the recognition of at least two species (*E. marmorata* and *E. pallida*), and a possible third based on populations in Baja California. However, they did not discuss in detail the morphological characters that would help to diagnose these species beyond those specified by Seeliger (1945). Given that these characters are somewhat variable within the proposed species, and that Holland (1992) described shell shape variation that might be consistent with this taxonomy, we wondered whether a geometric morphometric analysis of shell shape would provide a more reliable way of diagnosing groups (whether species or subspecies) within *E. marmorata*.

In this study, we attempt to estimate the best classification scheme of *E. marmorata* based on variation in plastral (ventral shell) shape in order to determine whether this character is consistent with any of the past divisions based on other morphological features or molecular data. Because of unclear geographic boundaries between subgroups of *E. marmorata*, we compare multiple hypotheses of morphologically- and molecularly-based classification. We hypothesize that if morphological variation corresponds to class assignment, then it should be possible to determine the best classification hypothesis of *E. marmorata* from amongst multiple candidate hypotheses. However, if morphological variation does not correspond to any classification hypothesis, then supervised learning model generalization performance will be poor and reflect how variation may not follow along with any of the candidate classification hypotheses.

## MATERIALS AND METHODS

## *Specimens, sampling, morphometrics*

We collected landmark-based morphometric data from 354 adult *E. marmorata* museum specimens. These specimens are a subset of those included in Angielczyk and Sheets (2007), Angielczyk et al. (2011), and Angielczyk and Feldman (2013) and represents adult individuals. We chose to focus on adults because significant changes in plastron shape occur over the course of ontogeny in *E. marmorata* and other emydines (Angielczyk and Feldman 2013).  
PETER NOTE – HOW WAS SOMETHING CLASSIFIED AS AN ADULT?

We assigned a classification to each specimen for the different binning schemes based on geographic occurrence data recorded in museum collection archives. When precise latitude and longitude information was not available we estimated it from whatever locality information was present. Because the specimens sampled to obtain the genetic data used to define the subclades were not available for study, all specimen classifications were based solely on the geographic information, not explicit assignment in previous studies. Because the exact barriers between different biogeographic regions are unknown and unclear, we represented each hypothesis with two different schemes; we compared a total of six different schemes. The schemes differed based on where geographic boundaries were assigned. This changes how certain individuals were assigned to one of the groups within in hypothesis such as which of the three morphologically defined groups, which of the four mitochondrially defined groups, and so on.

Following previous work on plastron variation (Angielczyk and Feldman 2013; Angielczyk et al. 2011; Angielczyk and Sheets 2007), we used TpsDig 2.04 (Rohlf 2005) to digitize 19 landmarks (Fig. 1). Seventeen of the landmarks are at the endpoints or intersection of the keratinous plastral scutes that cover the plastron. Twelve of the landmarks were symmetrical across the axis of symmetry and, in order to prevent issues surrounding degrees of freedom and other similar concerns (Klingenberg et al. 2002), we reflected these landmarks across the axis of symmetry (i.e. midline) prior to analysis and used the average position of each symmetrical pair. In cases where damage or incompleteness prevented symmetric landmarks from being determined, we used only the single member of the pair. We conducted all subsequent analyses on the resulting “half” plastra. We superimposed the plastral landmark configurations using generalized Procrustes analysis (Dryden and Mardia 1998), after which, we calculated the principal components (PC) of shape using the *shapes* package for R (Dryden 2013; R Core Team 2013).

## *Machine learning analyses*

*Unsupervised learning.*— In order to preserve the relationship between all landmark configurations in shape space, we measured the dissimilarity between observations using Kendall’s Riemannian shape distance or  $\rho$  (Dryden and Mardia 1998; Kendall 1984). We chose this metric because shape space, or the set of all possible shape configurations following Procrustes superimposition, is a Riemannian manifold and thus non-Euclidean (Dryden and Mardia

1998).  $\rho$  varies between 0 and  $\pi/2$  when there is no reflection invariance, which should not be  
a concern in the case of the half plastral landmark configurations used in the study.

We divisively clustered the shape dissimilarity matrix using partitioning around mediods  
clustering (PAM), a method similar to  $k$ -means clustering except that instead of minimizing  
the sum of squared Euclidean distances between observations and centroids, the sum of squared  
dissimilarities between observations and mediods is minimized (Kaufman and Rousseeuw  
1990). Because the optimal number of clusters of shape configurations in the study was  
unknown, being possibly three, four, or some other value, we estimated clustering solutions in  
which the number of clusters varied between one and eight. We computed clustering solutions  
using the gap statistic, which is a measure of goodness of clustering (Tibshirani et al. 2001).

We conducted this analysis using the `cluster` package for R (Maechler et al. 2013).

*Supervised learning.*— We used three different supervised learning, or classification, approaches:  
linear discriminate analysis, multinomial logistic regression, and random forests. Linear  
discriminate analysis, also known as canonical variate analysis, is commonly used in studies  
of geometric morphometric data (Mitteroecker and Bookstein 2011; Zelditch et al. 2004).  
The other two methods, however, are not. In all cases, the optimal number of PCs used as  
predictors was chosen via maximum within-sample AUC value, explained below.

Linear discriminate analysis (LDA) attempts to find a linear combination of predictors that  
best model two or more classes. LDA is very similar to PCA except that instead of finding  
the linear combination of features that maximize the amount of explained variance in the  
data, LDA maximizes the differences between classes. The results of this analysis produces a  
transformation matrix by which the original features can be transformed to reflect the best  
discrimination between the classes. In this study, we applied LDA to the eigenscores from a  
subset of the total number of PCs, ranging from two to 6 in increasing order of complexity.  
In total, this produced nine different LDA scaling matrices.

Multinomial logistic regression is an extension of logistic regression, where instead of a binary  
response there are three or more response classes (Venables and Ripley 2002). Similar to  
the odds ratios calculated from the coefficients of a logistic regression, the relative risk of a  
classification can be determined from the coefficients of the model.

Random forest models are an extension of classification and regression trees (CART) (Breiman  
2001; Breiman et al. 1984). The goal of CARTs are to use a series of different features (i.e.  
predictors) to estimate the class of an observation. In top-down induction of decision trees for  
each member of a given set of predictor variables, attribute value tests are used to estimate  
the differences between classes. This process, called recursive partitioning, is then repeated  
on each subset. The recursion continues until the resulting observations all share the same  
class or no more meaningful partitions are possible. The resulting model is a tree structure  
by which observations are classified at each intersection via the estimated cutoff points from  
the attribute tests made during model fitting.

In a random forest model, many CARTs are built from a random subsample of both the features and the observations (specimens). This process is then repeated many times and the parameters of the final model are chosen as the mode of estimates from the distribution of CARTs (Breiman 2001). In addition to classifying the observations, this procedure allows for the features to be ranked in order of importance. This is a generally useful property for studies in which the goal is to describe and model the differences between classes and the relative importance of different predictors.

In this analysis, we used 1000 subtrees to estimate the random forest model parameters. We estimated the best set of predictors necessary for each classification scheme was estimated using a recursive feature selection algorithm, and we chose the optimal number of PCs to include based on the AUC of the model. Following the backwards selection algorithm implemented in `caret` (Kuhn and Johnson 2013), the maximum number of features were included in the initial model, their importance ranked, and the AUC of the model calculated. The lowest ranked feature was then removed, and the AUC of the model recalculated. This was repeated until only one feature, remained. Because PCs were kept in order of importance and not in relation to the amount of variance each PC described, these means that the PCs are not included in the order of ascending eigenvalue.

In classification studies, such as this one, a common metric of performance is area under the receiver operating characteristic curve (AUC). AUC is an estimate of the relationship between the false positive and true positive rates, as opposed to just the true positive rate (accuracy). This relationship is especially useful in cases where misclassification needs to be minimized just as much as accurate classification, as in this study. AUC ranges between 0.5 and 1, with 0.5 indicating classification no better than random and 1 indicating perfect classification (Hastie et al. 2009).

The standard AUC calculation is defined for binary classifications, however in this application there are multiple categories. The alternative calculation that we used follows an all-against-one strategy where the individual AUC values for each class versus all others are averaged to produce a multiclass AUC (Hand and Till 2001). To estimate confidence intervals on the out-of-sample AUC values, we performed a nonparametric bootstrap in which the true and estimated classifications were resampled with replacement. This was done 1000 times.

The ultimate measure of model fit is accurately predicting the values of unobserved samples (Hastie et al. 2009; Kuhn and Johnson 2013). Within-sample performance is inherently biased upwards, so model evaluation requires overcoming this bias. With very large sample sizes, as in this study, part of the sample can be used as the “training set” and the remainder acts as the “testing set.” The former is used for fitting the model where as the later is used for measuring model performance, and this process is called model generalization. In this analysis, we used 75% of samples as the training set while the remaining 25% were used as the testing set.

It is common for some out of sample observations to be misclassified. This misclassification may be due to the model not accurately representing shape variance, systematic differences

between the training and test sets, or systematic differences between the accurately and  
inaccurately classified samples. Testing and training sets are determined completely at random  
within each class and with respect to shape. Results were not effected by changes in testing  
or training set assignment.

To determine if there were systematic differences between the correctly and incorrectly  
classified samples, we used a permutation test to estimate if the dissimilarity between the  
correctly and incorrectly classified individuals were significantly different from random. The  
group labels were permuted 1000 times and the distance between the new centroids was  
calculated. The number of permutations less than the empirical difference divided by 1000  
gives a  $p$ -value for the test. Significant results indicate that correctly and incorrectly classified  
specimens are systematically different. This was done only for classes where there were 10 or  
more observations.

## RESULTS

### *Unsupervised learning*

Comparison of gap statistic values from PAM clustering show that the optimal, minimal  
number of clusters is most likely one (Fig. 2). There is some ambiguity in choice because,  
although it is not statistically different from a solution with only one group, the solution with  
two groupings does have the greatest mean gap statistic. However, there is no geographical  
signal in the results of this clustering solution (Fig. 3). Because of this, we assert that this  
means that there is no means of naturally partitioning plastron shape into distinct subgroups  
with out reference to external information.

### *Supervised learning*

AUC-based model selection revealed some important patterns of variation and congruence  
between the classification schemes and the actual data. Generally, the best performing models  
tended to include as many PCs as possible 4). Note that the best random forest models  
were determined via recursive feature selection, so PCs were not included in order of percent  
variance explained. That almost all LDA and multinomial logistic regression models were as  
complex as possible indicates that the differences between the different groups within each  
classification scheme are very small.

As part of fitting a random forest model, a ranking of variable importance also is determined.  
Interestingly, the order of variable importance is not the same as the order of the PCs (5).  
This means that the variance describing the differences between the classes does not align  
with the major axes of variance (i.e. the PCs). This result would be the case if variation  
between classes was extremely fine grained and not a part of the principal form or function  
of the plastron, which makes sense given that the plastron is involved in both protection  
and hydrodynamics and not necessarily mate choice (Germano and Bury 2009; Holland 1992;



Lubcke and Wilson 2007; Rivera 2008). Moreover, this result is congruous with the results from the AUC-based model selection for the multinomial logistic regression and LDA models.

Observed AUC values for all of the optimal models are not exceptionally high (4). In most cases the different proposed classification schemes are generally poor descriptors of the observed variation. It appears that the data set is overwhelmed by noise, making any accurate classifications difficult at best. This observation is cemented with the generalizations of the models to the testing data set (6).

Mean AUC values for the model generalizations, in most cases, are approximately equal to the observed AUC values from the training data set (Table 1). The cases in which the AUC from the generalizations is less than the observed, indicate poor model fit and a poor classification scheme. AUC values from model generalization, or estimating testing data set membership, does not indicate a clear “best” classification scheme (Fig. 6). Although the scheme with two species has the greatest AUC point estimate for each modeling approach, this scheme is not significantly greater than any other except in some limited cases (e.g. LDA, Table 2). Differences in mean shape between correctly and incorrectly classified observations from test set frequently were statistically significant, though there are exceptions. Again, this test was to determine if the mean shapes were statistically different or not. The frequency of these results, however, is important because it means that the different models are poor predictors of class membership. This may be because differences in plastron shape do not align with the any of the hypothesized classification schemes.

## DISCUSSION

The results of this study indicate that there is no clear grouping of *E. marmorata* based on plastron shape.

The unsupervised learning results which indicate only a single group of observations being optimal is congruous with the results from the generalizations of the supervised learning models. The classification schemes used in the supervised learning models correspond, loosely, to unsupervised learning solutions with multiple groups. Because unsupervised learning solutions with multiple groups are poor descriptors of the observed variation, it is important to see this generally supported by the supervised learning results.

The results from fitting the various supervised learning models for each of the classification scheme generally shows that no one scheme is “best.” A possible explanation for this that the genetic divergence associated with (sub)speciation is either not based on plastron morphology or local selective pressures due to hydrological regime overwhelming any possible morphological divergence.

Both the low AUC values ( $< 0.9$ ) and the significant difference between the correctly and incorrectly classified observations support the conclusion that none of the hypothesized classification schemes are good descriptors of the observed plastral variation.

INSERT MORE TEXT HERE.

## BIBLIOGRAPHY

- 328 Angielczyk, K. D. and C. R. Feldman. 2013. Are diminutive turtles miniaturized? The  
ontogeny of plastron shape in emydine turtles. *Biological Journal of the Linnean Society*  
330 108:727–755.
- Angielczyk, K. D., C. R. Feldman, and G. R. Miller. 2011. Adaptive evolution of plastron  
332 shape in emydine turtles. *Evolution* 65:377–394.
- Angielczyk, K. D. and H. D. Sheets. 2007. Investigation of simulated tectonic deformation in  
334 fossils using geometric morphometrics. *Paleobiology* 33:125–148.
- Baylac, M., C. Villemant, and G. Simbolotti. 2003. Combining geometric morphometrics  
336 with pattern recognition for the investigation of species complexes. *Biological Journal of  
the Linnean Society* 80:89–98.
- 338 Bickford, D., D. J. Lohman, N. S. Sodhi, P. K. L. Ng, R. Meier, K. Winker, K. K. Ingram,  
and I. Das. 2007. Cryptic species as a window on diversity and conservation. *Trends in  
340 ecology & evolution* 22:148–55.
- Breiman, L. 2001. Random Forests. *Machine Learning* 45:5–32.
- 342 Breiman, L., J. Friedman, C. J. Stone, and R. A. Olshen. 1984. Classification and regression  
trees. Wadsworth International Group, Belmont.
- 344 Bury, R. B., D. J. Germano, and G. W. Bury. 2010. Population Structure and Growth of the  
Turtle *Actinemys marmorata* from the KlamathSiskiyou Ecoregion: Age, Not Size, Matters.  
346 *Copeia* 2010:443–451.
- Cardini, A., D. Nagorsen, P. O’Higgins, P. D. Polly, R. W. Thorington Jr, and P. Tongiorgi.  
348 2009. Detecting biological distinctiveness using geometric morphometrics: an example case  
from the Vancouver Island marmot. *Ethology Ecology & Evolution* 21:209–223.
- 350 Caumul, R. and P. D. Polly. 2005. Phylogenetic and environmental components of mor-  
phological variation: skull, mandible, and molar shape in marmots (*Marmota*, Rodentia).  
352 *Evolution; international journal of organic evolution* 59:2460–72.
- Clare, E. L. 2011. Cryptic species? Patterns of maternal and paternal gene flow in eight  
354 neotropical bats. *PloS one* 6:e21460.
- Demandt, M. H. and S. Bergek. 2009. Identification of cyprinid hybrids by using geometric  
356 morphometrics and microsatellites. *Journal of Applied Ichthyology* 25:695–701.
- Dobigny, G., L. Granjon, V. Aniskin, K. Ba, and V. Voloboulev. 2003. A new sigling species  
358 of *Taterillus* (Muridae, Gerbillinae) from West Africa. *Mammalian Biology* 68:299–316.
- Dryden, I. L. 2013. shapes: Statistical shape analysis. R package version 1.1-8.
- 360 Dryden, I. L. and K. Y. Mardia. 1998. Statistical shape analysis. Wiley, New York.

Eldredge, N. and S. J. Gould. 1972. Punctuated equilibria: an alternative to phyletic gradualism. Pages 82–115 *in* Models in Paleobiology (T. J. M. Schopf, ed.). Freeman Cooper, San Francisco.

Feldman, C. R. and J. F. Parham. 2002. Molecular phylogenetics of emydine turtles: taxonomic revision and the evolution of shell kinesis. *Molecular Phylogenetics and Evolution* 22:388–98.

Francoy, T. M., R. A. O. Silva, P. Nunes-Silva, C. Menezes, and V. L. Imperatriz-Fonseca. 2009. Gender identification of five genera of stingless bees (Apidae, Meliponini) based on wing morphology. *Genetics and molecular research* 8:207–214.

Fujita, M. K., A. D. Leaché, F. T. Burbrink, J. a. McGuire, and C. Moritz. 2012. Coalescent-based species delimitation in an integrative taxonomy. *Trends in ecology & evolution* 27:480–8.

Funk, W. C., M. Caminer, and S. R. Ron. 2012. High levels of cryptic species diversity uncovered in Amazonian frogs. *Proceedings of the Royal Society B: Biological Sciences* 279:1806–14.

Gaubert, P., P. J. Taylor, C. a. Fernandes, M. W. Bruford, and G. Veron. 2005. Patterns of cryptic hybridization revealed using an integrative approach: a case study on genets (Carnivora, Viverridae, *Genetta* spp.) from the southern African subregion. *Biological Journal of the Linnean Society* 86:11–33.

Germano, D. J. and R. B. Bury. 2009. Variation in body size, growth, and population structure of *Actinemys marmorata* from lentic and lotic habitats in Southern Oregon. *Journal of Herpetology* 43:510–520.

Germano, D. J. and G. B. Rathbun. 2008. Growth, population structure, and reproduction of western pond turtles (*Actinemys marmorata*) on the Central Coast of California. *Chelonian Conservation and Biology* 7:188–194.

Gould, S. J. and N. Eldredge. 1977. Punctuated equilibria: the tempo and mode of evolution reconsidered. *Paleobiology* 3:115–151.

Gündüz, I., M. Jaarola, C. Tez, C. Yenyurt, P. D. Polly, and J. B. Searle. 2007. Multigenic and morphometric differentiation of ground squirrels (*Spermophilus*, Scuridae, Rodentia) in Turkey, with a description of a new species. *Molecular phylogenetics and evolution* 43:916–35.

Hand, D. J. and R. J. Till. 2001. A Simple Generalisation of the Area Under the ROC Curve for Multiple Class Classification Problems. *Machine Learning* 45:171–186.

Hastie, T., R. Tibshirani, and J. Friedman. 2009. The elements of statistical learning: data mining, inference, and prediction. 2nd ed. Springer, New York.

Holland, D. C. 1992. Level and pattern in morphological variation: a phylogeographic study

of the western pond turtle (*Clemmys marmorata*). Ph.D. thesis University of Southwestern Louisiana.

Hunt, G. 2008. Gradual or pulsed evolution: when should punctuational explanations be preferred? *Paleobiology* 34:360–377.

Kaufman, L. and P. J. Rousseeuw. 1990. Finding groups in data : an introduction to cluster analysis. Wiley, New York.

Kendall, D. G. 1977. The diffusion of shape. *Advances in Applied Probability* 9:428–430.

Kendall, D. G. 1984. Shape Manifolds, Procrustean Metrics, and Complex Projective Spaces. *Bulletin of the London Mathematical Society* 16:81–121.

Klingenberg, C. P., M. Barluenga, and A. Meyer. 2002. Shape analysis of symmetric structures: quantifying variation among individuals and asymmetry. *Evolution* 56:1909–1920.

Kuhn, M. and K. Johnson. 2013. Applied predictive modeling. Springer, New York, NY.

Lubcke, G. M. and D. S. Wilson. 2007. Variation in shell morphology of the Western Pond Turtle (*Actinemys marmorata* Baird and Giarard) from three aquatic habitats in Northern California. *Journal of Herpetology* 41:107–114.

MacLeod, N. 2007. Automated taxon identification in systematics: theory, approaches and applications. CRC Press, Boca Raton.

Maechler, M., P. Rousseeuw, A. Struyf, M. Hubert, and K. Hornik. 2013. cluster: Cluster Analysis Basics and Extensions. R package version 1.14.4.

Mitrovski-Bogdanovic, A., A. Petrovic, M. Mitrovic, A. Ivanovic, V. Žikic, P. Starý, C. Vorburger, and v. Tomanovic. 2013. Identification of two cryptic species within the *Praon abjectum* group (Hymenoptera: Braconidae: Aphidiinae) using molecular markers and geometric morphometrics. *Annals of the entomological society of America* 106:170–180.

Mitteroecker, P. and F. Bookstein. 2011. Linear Discrimination, Ordination, and the Visualization of Selection Gradients in Modern Morphometrics. *Evolutionary Biology* 38:100–114.

Pfenninger, M. and K. Schwenk. 2007. Cryptic animal species are homogeneously distributed among taxa and biogeographical regions. *BMC evolutionary biology* 7:121.

Polly, P. D. 2003. Paleophylogeography of *Sorex araneus*: molar shape as a morphological marker for fossil shrews. *Mammalia* 68:233–243.

Polly, P. D. 2007. Phylogeographic differentiation in *Sorex araneus*: morphology in relation to geography and karyotype. *Russian Journal of Theriology* 6:73–84.

R Core Team. 2013. R: A Language and Environment for Statistical Computing. R Foundation for Statistical Computing Vienna, Austria.

Rivera, G. 2008. Ecomorphological variation in shell shape of the freshwater turtle *Pseudemys concinna* inhabiting different aquatic flow regimes. *Integrative and comparative biology* 48:769–87.

Rohlf, F. J. 2005. TpsDig 2.04.

Schilck-Steiner, B. C., B. Seifert, C. Stauffer, E. Christian, R. H. Crozier, and F. M. Steiner. 2007. Without morphology, cryptic species stay in taxonomic crypsis following discovery. *Trends in ecology & evolution* 22:391–392.

Seeliger, L. M. 1945. Variation in the Pacific Mud Turtle. *Copeia* 1945:150–159.

Spinks, P. Q. and H. B. Shaffer. 2005. Range-wide molecular analysis of the western pond turtle (*Emys marmorata*): cryptic variation, isolation by distance, and their conservation implications. *Molecular ecology* 14:2047–64.

Spinks, P. Q., R. C. Thomson, and H. Bradley Shaffer. 2014. The advantages of going large: genome wide SNPs clarify the complex population history and systematics of the threatened western pond turtle. *Molecular Ecology Pages* n/a–n/a.

Spinks, P. Q., R. C. Thomson, and H. B. Shaffer. 2010. Nuclear gene phylogeography reveals the historical legacy of an ancient inland sea on lineages of the western pond turtle, *Emys marmorata* in California. *Molecular ecology* 19:542–56.

Stuart, B. L., R. F. Inger, and H. K. Voris. 2006. High level of cryptic species diversity revealed by sympatric lineages of Southeast Asian forest frogs. *Biology letters* 2:470–4.

Sztencel-Jabonka, A., G. Jones, and W. Bogdanowicz. 2009. Skull Morphology of Two Cryptic Bat Species: *Pipistrellus pipistrellus* and *P. pygmaeus* A 3D Geometric Morphometrics Approach with Landmark Reconstruction. *Acta Chiropterologica* 11:113–126.

Tibshirani, R., G. Walther, and T. Hastie. 2001. Estimating the number of clusters in a data set via the gap statistic. *Journal of the Royal Statistical Society: Series B (Statistical Methodology)* 63:411–423.

Van Bocxlaer, B. and G. Hunt. 2013. Morphological stasis in an ongoing gastropod radiation from Lake Malawi. *Proceedings of the National Academy of Sciences* .

van den Brink, V. and F. Bokma. 2011. Morphometric shape analysis using learning vector quantization neural networks an example distinguishing two microtine vole species. *Annales Zoologici Fennici* 48:359–364.

Venables, W. and B. D. Ripley. 2002. *Modern applied statistics with S*. 4th ed. Springer, New York.

Yang, Z. and B. Rannala. 2010. Bayesian species delimitation using multilocus sequence data. *Proceedings of the National Academy of Sciences* 107:9264–9.

464 Zelditch, M. L., D. L. Swiderski, and H. D. Sheets. 2004. Geometric morphometrics for  
biologists: a primer. Elsevier Academic Press, Amsterdam.

Scheme	random forest		multinomial logistic regression		linear discriminate analysis	
	Observed	Generalized	Observed	Generalized	Observed	Generalized
Morphology 1	0.63	0.73	0.75	0.79	0.75	0.80
Morphology 2	0.61	0.58	0.76	0.77	0.76	0.77
Mitochondria 1	0.63	0.62	0.75	0.63	0.75	0.63
Mitochondria 2	0.77	0.67	0.80	0.64	0.80	0.63
Mitochondria 3	0.56	0.64	0.71	0.74	0.71	0.73
Nuclear	0.56	0.67	0.74	0.62	0.74	0.77

Table 1: AUC values for the best model of each classification scheme for both the observed (training) data and the generalized (testing) data. Results from all three different supervised learning approaches are shown here. AUC values range between 0.5 and 1.

(a) random forest

Scheme	P(best - other > 0)
sh1	*
sh2	0.79
sh3	0.89
sh4	0.79
sh5	0.82
spinks	0.79

(b) multinomial logistic regression

Scheme	P(best - other > 0)
sh1	*
sh2	0.55
sh3	0.94
sh4	0.96
sh5	0.57
spinks	0.69

(c) linear discriminate analysis

Scheme	P(best - other > 0)
sh1	1
sh2	1
sh3	1
sh4	0.96
sh5	*
spinks	0.73

Table 2: Results of bootstrap comparisons between the scheme with the highest mean AUC value and all other schemes. An asterix indicates the best scheme. This was done for each of the three modeling techniques included in this study. Probabilities are the percent of comparisons that are greater than the observed difference in means.



## (a) random forest

Scheme	Class	distance	P(distance - simulated > 0)
sh1	CCR	1.59	0.77
	marm	2.06	0.87
sh2	CCR	1.81	0.88
	marm	2.16	1.00
sh3	CCR	2.37	0.94
	marm	2.37	0.99
sh4	marm	2.07	1.00
	pall	2.13	0.99
sh5	marm	1.91	0.85
	pall	2.00	0.94
spinks	1	1.79	0.40
	3	3.30	0.97

## (b) multinomial logistic regression

Scheme	Class	distance	P(distance - simulated > 0)
sh1	CCR	2.06	1.00
	marm	2.22	0.93
sh2	CCR	2.50	1.00
	marm	2.60	1.00
sh3	CCR	2.39	0.99
	marm	2.24	0.98
sh4	marm	2.23	1.00
	pall	2.15	1.00
sh5	marm	2.43	0.97
	pall	2.60	1.00
spinks	1	2.96	0.92
	3	3.18	0.99

## (c) linear discriminate analysis

Scheme	Class	distance	P(distance - simulated > 0)
sh1	CCR	2.07	1.00
	marm	2.22	1.00
sh2	CCR	2.20	1.00
	marm	1.87	0.98
sh3	CCR	2.75	0.98
	marm	2.36	0.47
sh4	marm	2.23	1.00
	pall	2.15	1.00
sh5	marm	2.43	0.96
	pall	2.60	1.00
spinks	1	2.96	0.90
	3	3.33	1.00

Table 3: Results of comparisons between correctly and incorrectly classified observations from the testing data set. For each scheme, the classifications with at least 10 observations were tested. This was done for each of the three modeling techniques included in this study.

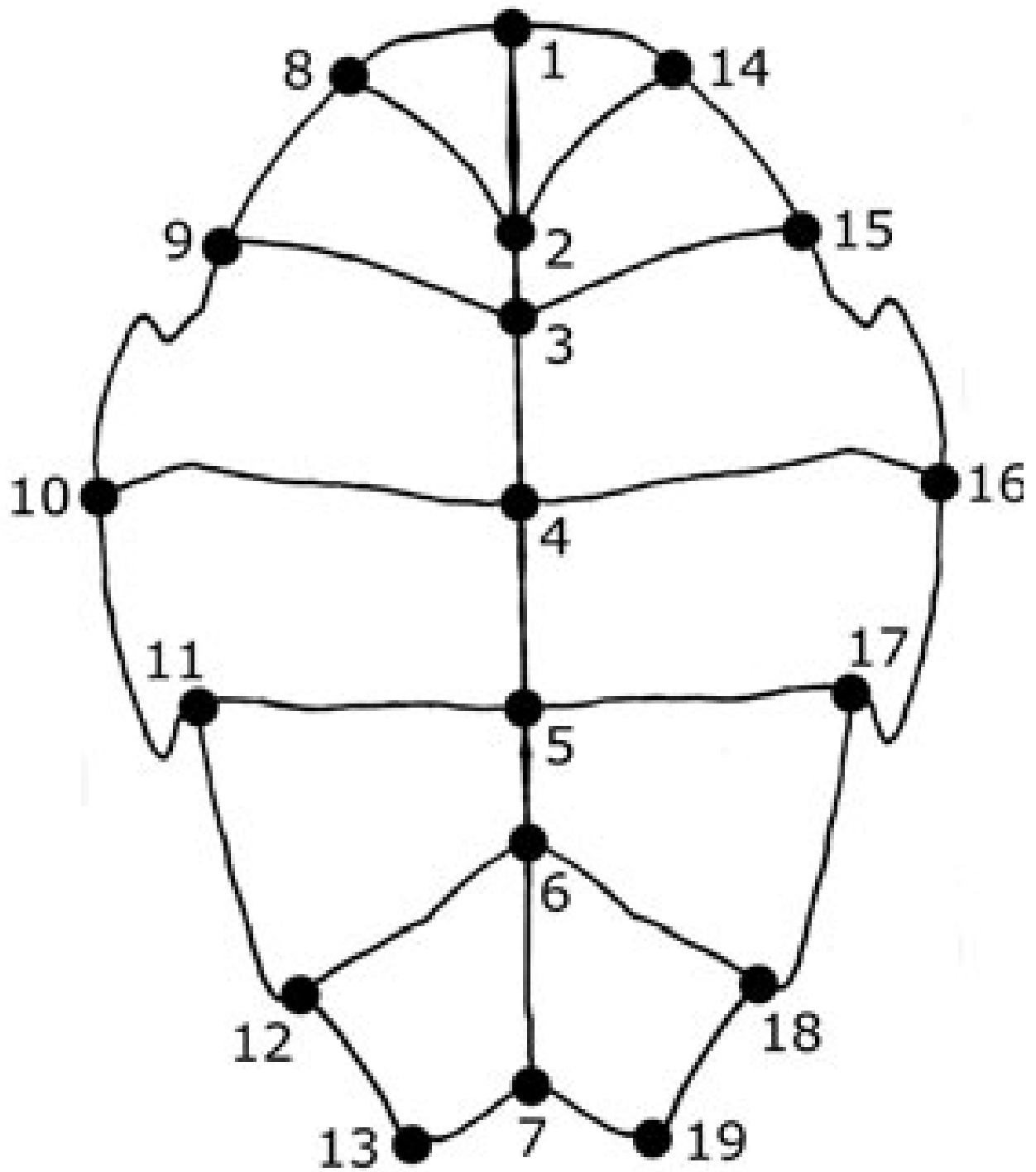


Figure 1: Depiction of general plastral shape of *E. marmorata* and position of the 19 landmark used in this study. Anterior is towards the top of the figure.

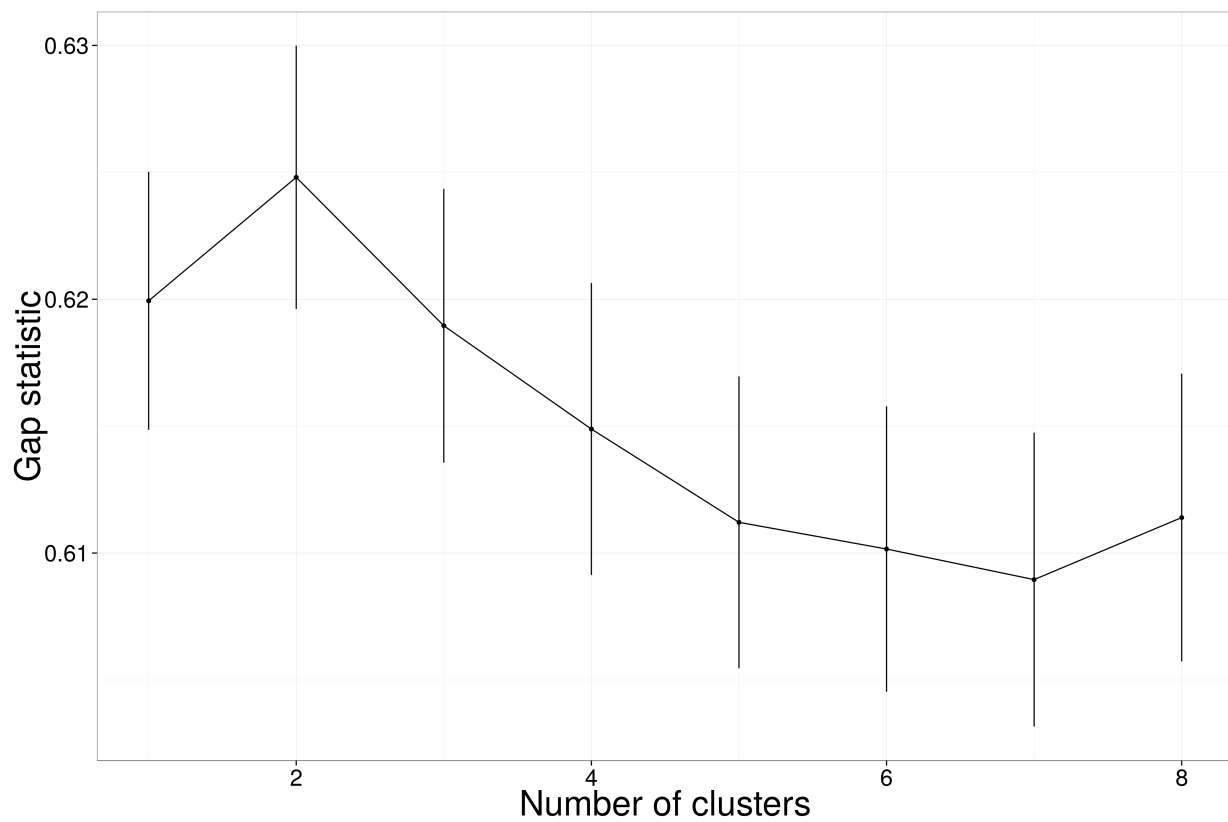


Figure 2: Results from PAM clustering of the Riemannian shape distance for 8 different number of clusters. Vertical lines are 1 standard deviation of the mean determined from 500 resamples.

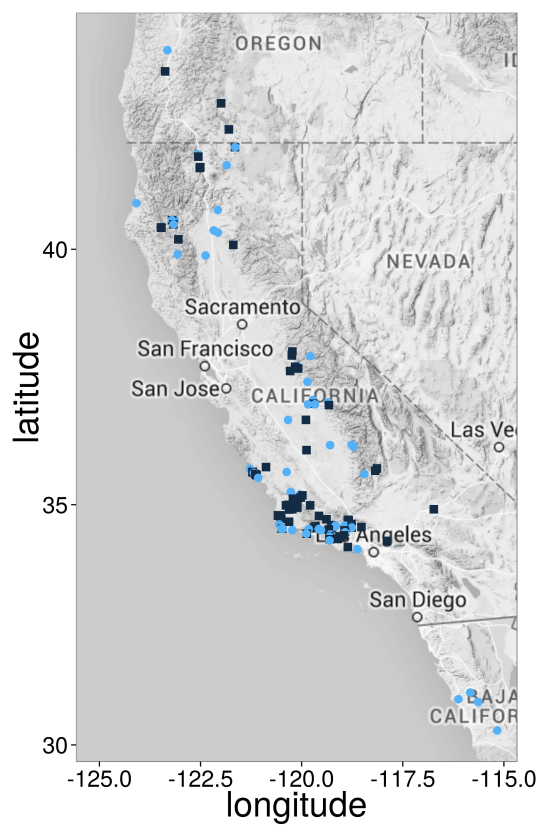


Figure 3: Comparison of geographic distribution of clustered observations from the 2 clustering PAM solution. Colour and shape correspond to each of the groups. There is clearly no geographic signal in the data.

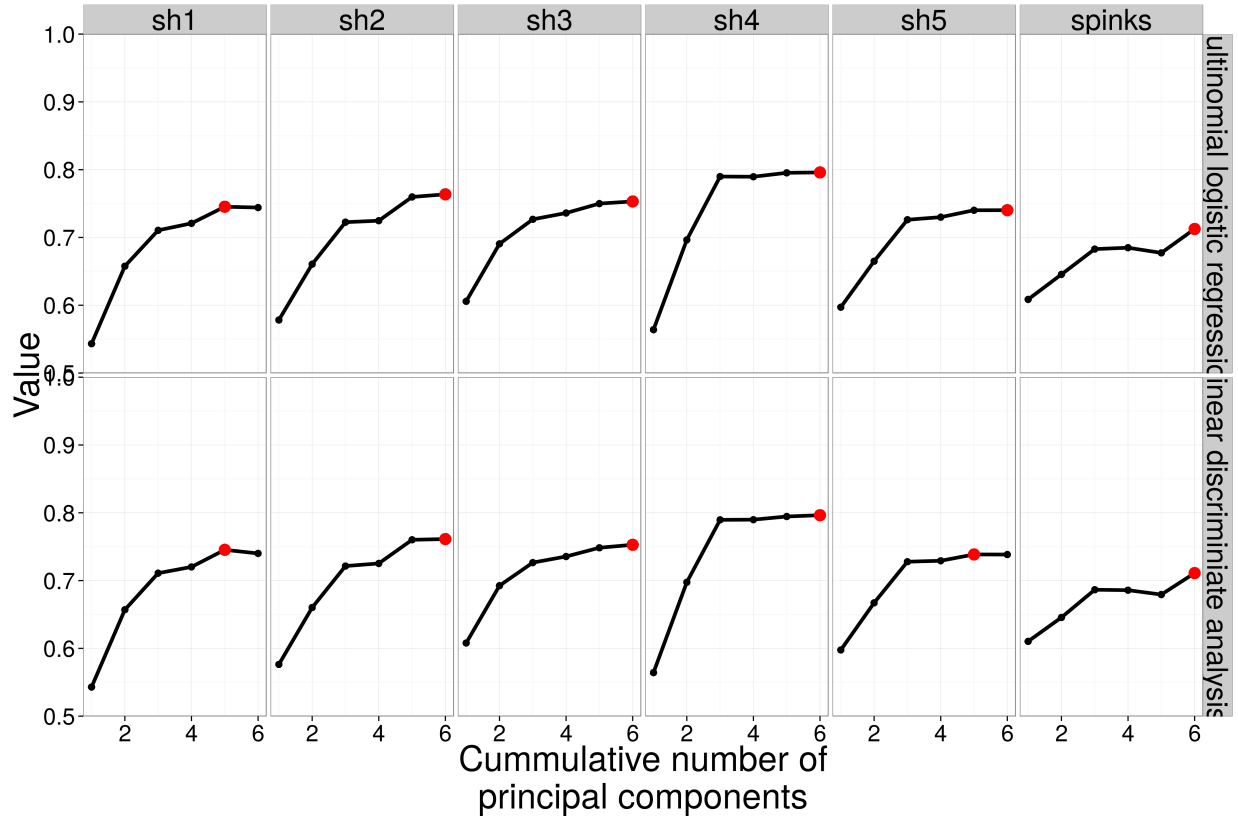


Figure 4: Graphical representation of the AUC values from model selection for multinomial logistic regression and linear discriminate analysis, respectively. AUC model selection is based on greatest AUC value. The horizontal axis corresponds to the cumulative number of axes included in the model of interest. A red dot corresponds to the AUC best model for that classification scheme.

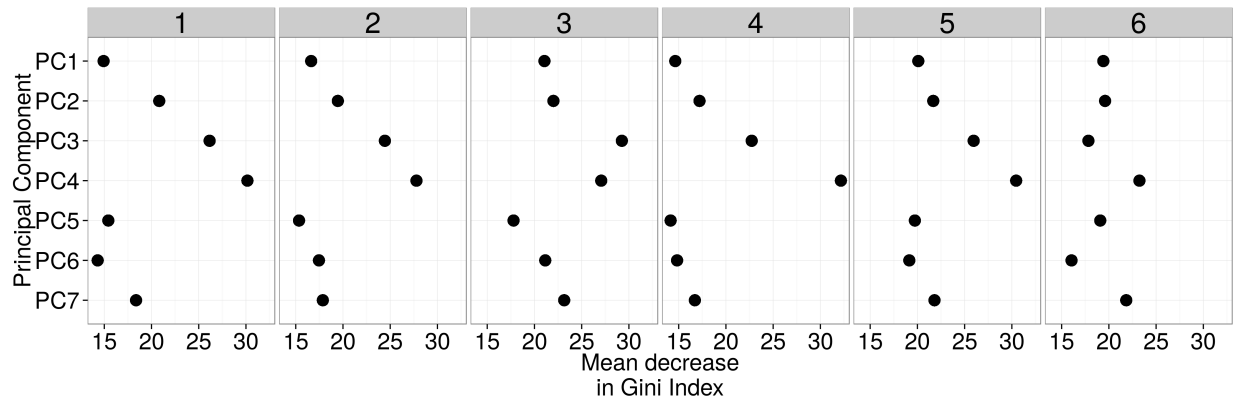


Figure 5: Variable importance from the random forest models for each of the six classification schemes. Importance is measured as the mean decrease in Gini Index, which is a measure of the strength by which that variable determines CART structure. Indices that are farther to the right indicate greater variable importance.

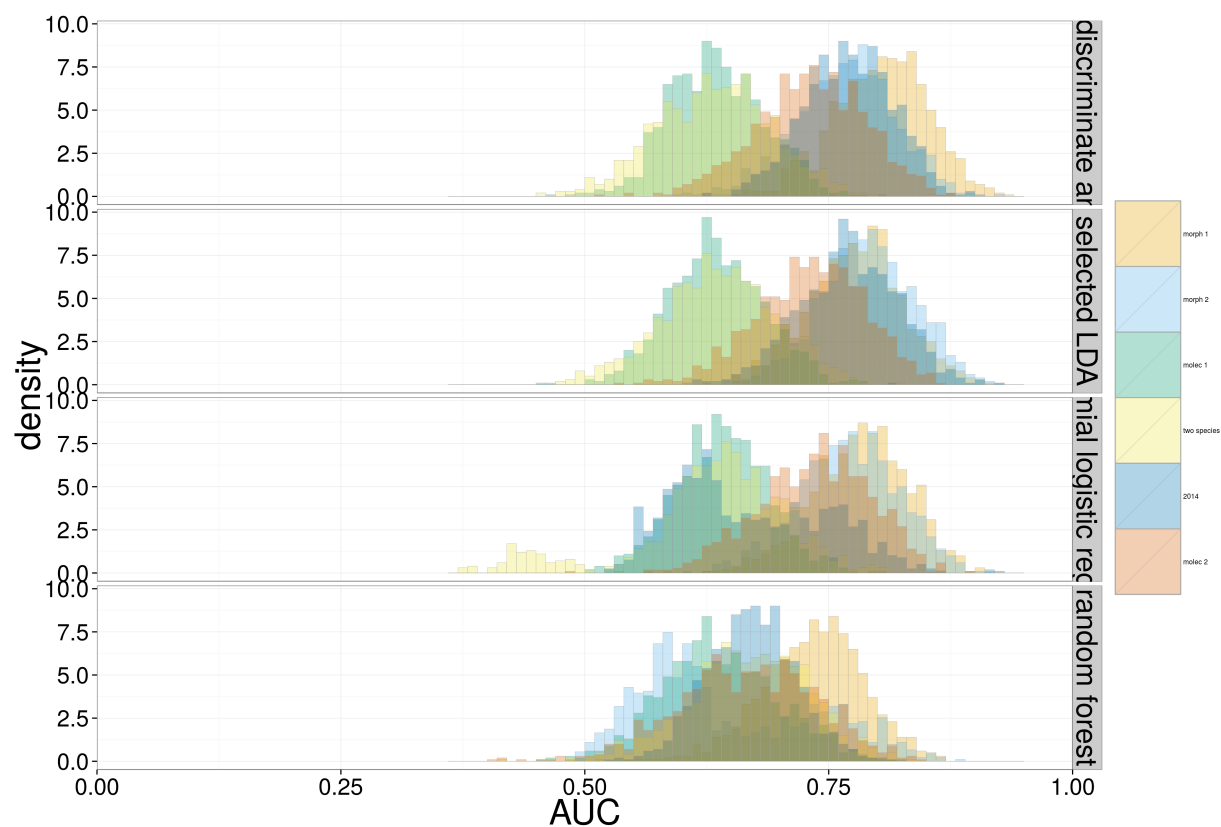


Figure 6: Bootstrap distributions for generalized AUC values for each of the classification schemes. Each row corresponds to a different modeling approach: LDA, LDA using best variables from random forest, multinomial logistic regression, and random forest. Each distribution corresponds to 1000 bootstrap replicates.